Population Shape Regression From Random Design Data

B. C. Davis
University of North Carolina at Chapel Hill
Chapel Hill, NC, USA
Kitware, Inc.
Clifton Park, NY, USA
brad.davis@unc.edu

P. T. Fletcher
University of Utah
Salt Lake City, Utah, USA

E. Bullitt
University of North Carolina at Chapel Hill
Chapel Hill, NC, USA

S. Joshi
University of Utah
Salt Lake City, Utah, USA

Abstract

Regression analysis is a powerful tool for the study of changes in a dependent variable as a function of an independent regressor variable, and in particular it is applicable to the study of anatomical growth and shape change. When the underlying process can be modeled by parameters in a Euclidean space, classical regression techniques [13, 34] are applicable and have been studied extensively. However, recent work suggests that attempts to describe anatomical shapes using flat Euclidean spaces *undermines our ability to represent natural biological variability [9, 11].*

In this paper we develop a method for regression analysis of general, manifold-valued data. Specifically, we extend Nadaraya-Watson kernel regression by recasting the regression problem in terms of Fréchet expectation. Although this method is quite general, our driving problem is the study anatomical shape change as a function of age from random design image data.

We demonstrate our method by analyzing shape change in the brain from a random design dataset of MR images of 89 healthy adults ranging in age from 22 to 79 years. To study the small scale changes in anatomy, we use the infinite dimensional manifold of diffeomorphic transformations, with an associated metric. We regress a representative anatomical shape, as a function of age, from this population.

1. Introduction

An important area of medical image analysis is the development of methods for automated and computer-assisted assessment of anatomical change over time. For example, the analysis of structural brain change over time is important for understanding healthy aging. These methods also provide markers for understanding disease progression.

A number of longitudinal growth models have been developed to provide this type of analysis to time-series imagery of a single subject (e.g., [2, 7, 24, 32]). While these methods provide important results, their use is limited by their reliance on longitudinal data, which can be impractical to obtain for many medical studies. Also, while these methods allow for the study of an *individual's* anatomy over time, they do not apply when the *average* growth for a population is of interest.

Random design data sets, which contain anatomical data from many different individuals, provide a rich environment for addressing these problems. However, in order to detect time-related trends in such data, two distinct aspects of anatomical variation must be separated: individual variation and time effect. For measurements that naturally form Euclidean vector spaces, this separation can be achieved by *regressing* a representative value over time from the data.

For example, in Figure 1 we apply kernel regression to measurements reported in a study by Mortamet et al. [28] on the effect of aging on gray matter and ventricle volume in the brain. The regression curves demonstrate the average volume, as a function of patient age, of these structures. These trends—on average there is a loss of gray matter and expansion of the ventricles—have been widely reported in the medical literature on aging [12, 23, 28]. While volume-based regression analysis is important, it does not provide any information about the detailed *shape* changes that occur in the brain, on average, as a function of age. This has motivated us to study regression of shapes.

Recent work has suggested that representing the geome-

try of shapes in *flat Euclidean vector spaces* limits our ability to represent natural variability in populations [9, 11, 24]. For example, Figure 2 demonstrates the amazing *non-linear* variability in brain shape among a population of healthy adults. The analysis of transformation groups that describe shape change are essential to understanding this shape variability. These groups vary in dimensionality from simple rigid rotations to the infinite-dimensional group of diffeomorphisms [26]. These groups are not generally vector spaces and are instead naturally represented as manifolds.

A number of authors have contributed to the field of statistical analysis on manifolds (see Pennec [30] for a more detailed history). Early work on manifold statistics includes directional statistics [5, 16] and statistics of point set shape spaces [19, 20]. The large sample properties of sample means on manifolds are developed in [3, 4]. Jupp and Kent [17] describe a method of regression of spherical data that 'unwraps' the data onto a tangent plane, where standard curve fitting methods can be applied. In [9, 14, 30], statistical concepts such as averaging and principal components analysis were extended to manifolds representing anatomical shape variability. Many of the ideas are based on the method of averaging in metric spaces proposed by Fréchet [10].

In this paper we use the notion of Fréchet expectation to generalize regression to manifold-valued data. We use this method to study spatio-temporal anatomical shape change in a random design database consisting of three-dimensional MR images of healthy adults. Our method generalizes Nadaraya-Watson kernel regression in order to compute representative images of this population over time. To determine the shape change in the population over time, we apply a diffeomorphic growth model [24] to this time-indexed population representative image.

2. Methods

2.1. Review of univariate kernel regression

Univariate kernel regression [13, 34] is a non-parametric method used to estimate the relationship, on average, between an independent random variable T and a dependent random variable Y. The estimation is based on a set of observations $\{t_i, y_i\}_{i=1}^N$ drawn from the joint distribution of T and Y. This relationship between T and Y can be modeled as $y_i = m(t_i) + \epsilon_i$, where ϵ_i describes the random error of the model for the ith observation and m is the unknown function that is to be estimated.

In this setting, $m(t)$ is defined by the conditional expectation

$$m(t) \equiv E(Y|T=t) = \int y \frac{f(t,y)}{f_T(t)}\, dy \qquad (1)$$

where $f_T(t)$ is the marginal density of T and $f(t,y)$ is the joint density function of T and Y. For random design data, both $f(t,y)$ and $f_T(t)$ are unknown and so m has no closed-form solution. A number of estimators for m have been proposed in the kernel regression literature.

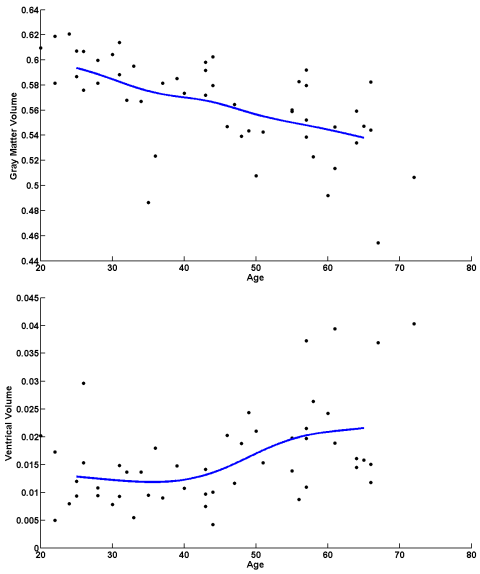

Figure 1. Illustration of univariate kernel regression: the effect of aging on gray matter (top) and ventricle volume (bottom) in the brain. Circles represent volume measurements relative to total brain volume. Kernel regression is used to estimate the relationship between patient age and structure volume (filled lines).

One such estimator—the Nadaraya-Watson kernel regression estimator [29, 35]—can be derived from (1) by replacing the unknown densities with their kernel density estimates

$$\hat{f}_T^h(t) \equiv \frac{1}{N}\sum_{i=1}^{N} K_h(t-t_i) \qquad (2)$$

and

$$\hat{f}^{h,g}(t,y) \equiv \frac{1}{N}\sum_{i=1}^{N} K_h(t-t_i)K_g(y-y_i). \qquad (3)$$

In these equations, K is a function that satisfies $\int_{\mathbb{R}} K(t)\,dt = 1$. $K_h(t) \equiv \frac{1}{h}K(\frac{t}{h})$ and $K_g(t) \equiv \frac{1}{g}K(\frac{t}{g})$ are kernel functions with bandwidths h and g respectively.

Plugging these density estimates into equation 1 gives

$$\hat{m}_{h,g}(t) = \int y \frac{\frac{1}{N}\sum_{i=1}^{N} K_h(t-t_i)K_g(y-y_i)}{\frac{1}{N}\sum_{i=1}^{N} K_h(t-t_i)}\, dy. \qquad (4)$$

Finally, assuming that K is symmetric about the origin, integration of the numerator leads to

$$\hat{m}_h(t) = \frac{\sum_{i=1}^{N} K_h(t-t_i)y_i}{\sum_{i=1}^{N} K_h(t-t_i)}. \qquad (5)$$

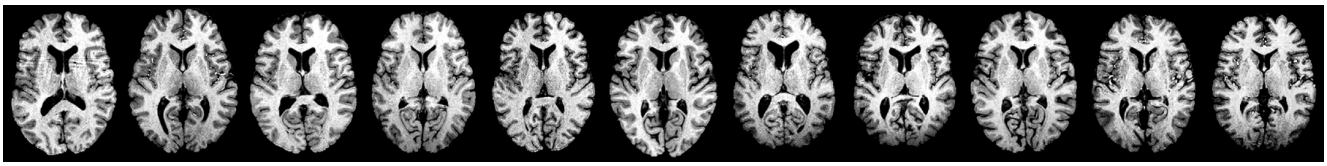

Figure 2. To demonstrate the extent of natural brain shape variability within a population of healthy subjects, a mid-axial slice is presented for a sample of images used in this study. The images are arranged in order of increasing patient age from 40 (left) to 50 (right). Because of the complexity of the shapes and the high level of natural shape variability, it is extremely difficult to visually discern any patterns within these data.

Intuitively, the Nadaraya-Watson estimator returns the weighted average of the observations y_i, with the weighting determined by the kernel. Note that $\hat{f}^{h,g}(t,y)$ is factored out of the estimator—the weights only depend on the values t_i.

In Figure 1 we illustrate univariate kernel regression by applying it to demonstrate the effect of aging on ventricle volume and gray matter volume in the brain. This illustration is based on data collected by Mortamet et al. [28]. Each cross-mark represents a volume measurement, relative to total brain volume, for a particular patient. These measurements were derived from 3D MR images of 50 healthy adults ranging in age from 20 to 72 using an expectation-maximization based automatic segmentation method [21]. We used kernel regression to estimate the relationship, on average, between volume and patient age (filled lines). A Nadaraya-Watson kernel estimator with a Gaussian kernel of width $\sigma = 6$ years was used.

2.2. Kernel regression on Riemannian manifolds

In this section we consider the regression problem in the more general setting of manifold-valued observations. Let $\{t_i, p_i\}_{i=1}^N$ be a collection of observations where the t_i are drawn from a univariate random variable T, but where p_i are points on a Riemannian manifold $\mathcal{M}$. The classical kernel regression methods presented in Section 2.1 are not applicable in this setting because they rely on the vector space structure of the observations. In particular, the addition operator in (5) is not well defined.

The goal is to determine the relationship, on average, between the independent variable T and the distribution of the points $\{p_i\}$ on the manifold. This relationship can be modeled by

$$p_i = \mathrm{Exp}_{m(t_i)}(\epsilon_i) \tag{6}$$

where $m : \mathbb{R} \to \mathcal{M}$ defines a curve on $\mathcal{M}$. The error term $\epsilon_i \in T_{m(t_i)}\mathcal{M}$ is a tangent vector that is interpreted as the displacement along the manifold of each observation p_i from the curve $m(t)$. The exponential mapping, Exp, returns the point on $\mathcal{M}$ at time one along the geodesic flow beginning at $m(t_i)$ with initial velocity ϵ_i.

Following the univariate case, we define the regression function $m(t)$ in terms of expectation. However, in this case we generalize the idea of expectation of real random variables to manifold-valued random variables via Fréchet expectation [10, 18]. Let $f(p), p \in \mathcal{M}$ be a probability density on the manifold. The Fréchet expectation is defined as

$$\mathbb{E}_f[p] \equiv \operatorname*{argmin}_{q \in \mathcal{M}} \int_{\mathcal{M}} d(q,p)^2 f(p) \tag{7}$$

where $d(q,m)$ is the metric on the manifold $\mathcal{M}$. This definition is motivated by a minimum variance characterization of the mean, where variance is defined in terms of the metric. Note that Fréchet expectation might not be unique [18]. Using the above definition, an empirical estimate of the Fréchet mean, given a collection of observations $\{p_i, i = 1 \cdots N\}$ on a manifold $\mathcal{M}$, is defined by

$$\mu = \operatorname*{argmin}_{q \in \mathcal{M}} \frac{1}{N} \sum_{i}^{N} d(q,p_i)^2.$$

Motivated by the definition of the Nadaraya-Watson estimator as a weighted averaging, we define a *manifold kernel regression estimator* using the weighted Fréchet empirical mean estimator as

$$\hat{m}_h(t) = \operatorname*{argmin}_{q \in \mathcal{M}} \left(\frac{\sum_{i=1}^N K_h(t-t_i) d(q,p_i)^2}{\sum_{i=1}^N K_h(t-t_i)} \right). \tag{8}$$

Notice that when the manifold under study is a Euclidean vector space, equipped with the standard Euclidean norm, the above minimization results in the Nadaraya-Watson estimator.

2.3. Regression of rotational pose ($SO(3)$)

Before we present results of the study of brain growth, we exemplify the methodology in detail on the finite-dimensional Lie group of 3D rotations, $SO(3)$.

Following the approach in [6], we solve the weighted averaging problem in (8) by a gradient descent algorithm. The tangent space of $SO(3)$ at the identity is the Lie algebra of 3×3 skew-symmetric matrices, denoted $\mathfrak{so}(3)$. We equip

$SO(3)$ with the standard bi-invariant metric, given by the Frobenius inner product on $\mathfrak{so}(3)$. The tangent space at an arbitrary rotation $R \in SO(3)$ is given by either left or right multiplication of $\mathfrak{so}(3)$ by R.

The Lie group exponential map and its inverse, the log map, are used to compute geodesics and distances. The exponential map for a tangent vector $X \in \mathfrak{so}(3)$ is given by

$$\exp(X) = \begin{cases} I, & \theta = 0, \\ I + \dfrac{\sin\theta}{\theta} X + \dfrac{1-\cos\theta}{\theta^2} X^2, & \theta \in (0, \pi), \end{cases}$$

where $\theta = \sqrt{\frac{1}{2}\operatorname{tr}(X^T X)}$. A geodesic $\gamma(t)$ starting at a point $R \in SO(3)$ with initial velocity RX is given by $\gamma(t) = R\exp(tX)$. The Lie group log map for a rotation matrix $R \in SO(3)$ is given by

$$\log(R) = \begin{cases} I, & \theta = 0, \\ \dfrac{\theta}{2\sin\theta}(R - R^T), & |\theta| \in (0, \pi), \end{cases}$$

where $\operatorname{tr}(R) = 2\cos\theta + 1$. The distance between two rotations $R_1, R_2 \in SO(3)$ is given by $d(R_1, R_2) = \|\log(R_1^{-1} R_2)\|$.

Now consider the weighted averaging problem with rotation data $R_i \in SO(3)$ and corresponding weights $w_i = K_h(t - t_i)/\sum_{j=1}^N K_h(t - t_j)$. The regression problem in (8) minimizes the weighted sum-of-squared distance function of the form $f(R, \{R_i, w_i\}) = \sum_i w_i d(R, R_i)^2$. The gradient for this function at a point $R \in SO(3)$ is given by $\nabla_R f = -\sum_i w_i R \log(R^{-1} R_i)$. Therefore, given the estimate $\hat{R}_k$ for the weighted average, the gradient descent update to solve (8) is given by $\hat{R}_{k+1} = \hat{R}\exp(-R^{-1}\nabla_{\hat{R}_k} f)$.

2.4. Kernel regression for populations of brain images

In this section we apply our shape regression methodology to study the effect of aging on brain *shape* from random design image data. We have observations of the form $\{t_i, I_i\}_{i=1}^N$ where t_i is the age of patient i and I_i is a three-dimensional image that we identify with the anatomical configuration of patient i. We seek the unknown function m that associates a representative anatomical configuration, and its associated image $\hat{I}$, with each age.

It is important to point out that we cannot rely on the natural L^2 structure of the images themselves for our analysis. While images can be added voxel-wise, the result is a loss of any identification with the anatomical configuration. Instead, we represent anatomical differences in terms of transformations of the underlying image coordinates. This approach is common within the shape analysis literature [11, 25]. Because we are interested in capturing the large, natural geometric variability evident in the brain (cf. Figure 2), we represent shape change as the action of the group of diffeomorphisms, denoted by $\mathcal{H}$. In the rest of this section, we formalize this notion and define a distance between shapes that is valid in this setting and will allow us to apply our regression methodology.

Let $\Omega \subset \mathbb{R}^3$ be the underlying coordinate system of the observed images I_i. Each image $I \in \mathcal{I}$ can be formally defined as an L^2 function from Ω to the reals. Let $\mathcal{H}$ be the group of diffeomorphisms that are isotopic to the identity. Each element $\phi : \Omega \to \Omega$ in $\mathcal{H}$ deforms an image according to the following rule

$$I_\phi(x) = I(\phi^{-1}(x)). \tag{9}$$

We apply the theory of large deformation diffeomorphisms [1, 8, 15, 26] to generate deformations ϕ that are solutions to the Lagrangian ODEs $\frac{d}{ds}\phi_s(x) = v_s(\phi_s(x))$ for a simulated time parameter $s \in [0, 1]$. The transformations are generated by integrating the velocity fields v forward in time.

We introduce a metric on $\mathcal{H}$ using a Sobelev norm via a partial differential operator L applied to v. Let $e \in \mathcal{H}$ be the identity transformation. We define the squared metric $d_{\mathcal{H}}(e, \phi)^2$ as

$$d_{\mathcal{H}}(e, \phi)^2 = \min_{v : \dot{\phi}_s = v_s(\phi_s)} \int_0^1 \int_\Omega ||Lv_s(x)||^2 \, dx \, ds \tag{10}$$

subject to

$$\phi(x) = x + \int_0^1 v_s(\phi_s(x)) \, ds. \tag{11}$$

The distance between any two diffeomorphisms is defined by

$$d_{\mathcal{H}}(\phi_1, \phi_2)^2 = d_{\mathcal{H}}(e, \phi_1^{-1} \circ \phi_2)^2. \tag{12}$$

This distance satisfies all of the properties of a metric: it is non-negative, symmetric, and satisfies the triangle inequality[27].

Using this metric on $\mathcal{H}$, we can define the distance between two images as

$$\begin{aligned} d_{\mathcal{I}}(I_1, I_2)^2 \equiv & \\ & \min_{v : \dot{\phi}_s = v_s(\phi_s)} \int_0^1 \int_\Omega \|Lv_s(x)\|^2 \, dx \, ds \\ & + \frac{1}{\sigma^2} \int_\Omega \|I_1(\phi^{-1}(x)) - I_2(x)\|^2 \, dx \end{aligned} \tag{13}$$

where the second term accounts for the noise model of the image [14]. While this construction is motivated by the metric on $\mathcal{H}$, it does not strictly define Riemannian metric on the space of anatomical images (because of the second term). In the future we plan to define distance in terms of the elegant construction described in [33].

Having defined a metric on the space of images that accommodates anatomical variability, we can apply that metric to regress a representative anatomical configuration, with associated image, from our observations $\{t_i, I_i\}$

$$\hat{I}_h(t) = \underset{I \in \mathcal{I}}{\operatorname{argmin}} \left(\frac{\sum_{i=1}^{N} K_h(t - t_i) d(I, I_i)^2}{\sum_{i=1}^{N} K_h(t - t_i)} \right). \quad (14)$$

Equation 14 expresses the following intuitive idea: For any age t, the population can be represented by the anatomical configuration that is centrally located, according to d, among the observations that occur near in time to t. As in the univariate case, the weights are determined by the kernel K.

2.5. Diffeomorphic growth model

Having regressed a population representative anatomical image, as a function of age, we can now study the local shape changes evident—for the population—as a function of age. We apply the longitudinal growth model of Miller et al. [24] to the regressed image $\hat{I}(t)$ in order to estimate the time-indexed deformation that quantifies the fine scale anatomical shape change of $\hat{I}$ as a function of time.

2.6. Computational Strategy

We approximate the solution to (14) using an iterative greedy algorithm that is similar to the method described in [14]. When computing each representative image $\hat{I}(x)$, we use a multi-resolution approach that generates images at progressively higher resolutions, where each level is initialized by the results at the next coarsest scale. This strategy has the dual benefits of (a) addressing the large scale shape changes first and (b) speeding algorithm convergence.

The dominating computation at each iteration is a Fast Fourier Transform. The order of the algorithm is $MNn \log n$ where M is the number of iterations, N is the number of images, and n is the number of voxels along the largest dimension of the images. Therefore, the complexity grows linearly with the number of observations, making this algorithm suitable for application to large data sets.

3. Results

To demonstrate our method for estimating cross-sectional growth, we applied the algorithm to a database of 3D MR images. The database contains MRA, T1-FLASH, T1-MPRAGE, and T2-weighted images from 97 healthy adults ranging in age from 20 to 79 [22]. For this study we only utilized the T1-FLASH images; these images were acquired at a spatial resolution of 1mm$\times$1mm$\times$1mm using a 3 Tesla head-only scanner. The tissue exterior to the brain was removed using a mask generated by a brain segmentation tool described in [31]. This tool was also used for bias correction. In the final preprocessing step, all of the images were spatially aligned to an atlas using affine registration.

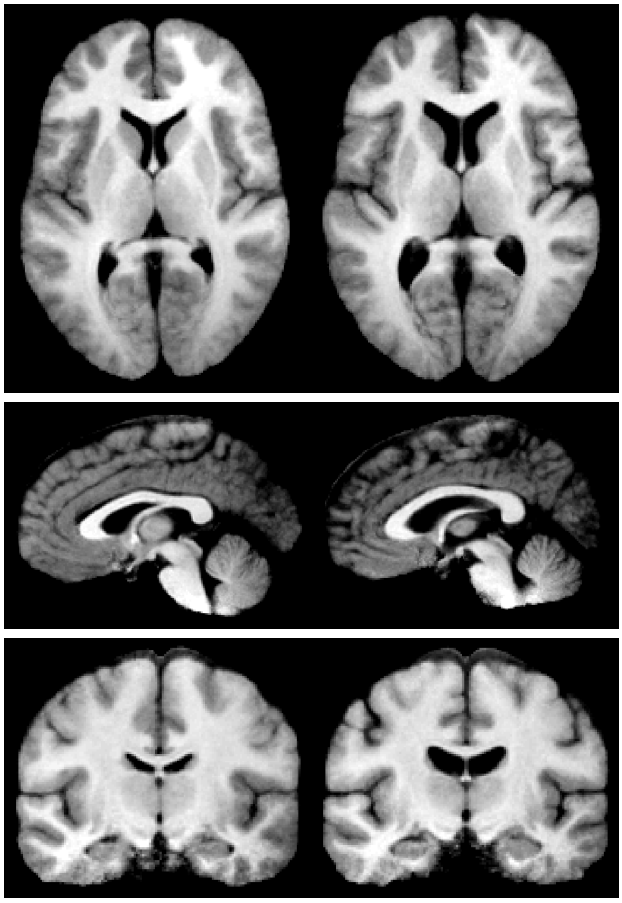

Figure 3. Representative anatomical images for the female cohort at ages 35 (left) and 55 (right). These images were generated from the random design 3D MR database using the shape regression method described in Section 2.

We applied our algorithm separately for males and females. We selected only patients for which T1-Flash data was available. The final size of the male cohort was 43 patients ranging in age from 22 to 79; the final size of the female cohort was 46 patients ranging in age from 22 to 68.

We applied the manifold kernel regression estimator (14) to compute representative anatomical images for each cohort. Images were computed for ages 35 to 55 at increments of 2 years using a Gaussian kernel with $\sigma = 5$ years. Figures 3 and 4 contain slices from these representative images for the female cohort. Each 3D image took approximately 4 hours to produce on a 2.4GHz system with approximately 16 gigabytes of RAM.

We applied the diffeomorphic growth estimation algorithm described in Section 2.5 to determine the anatomical shape change over time for each cohort. Figure 5 illustrates the instantaneous change in the deformation at ages

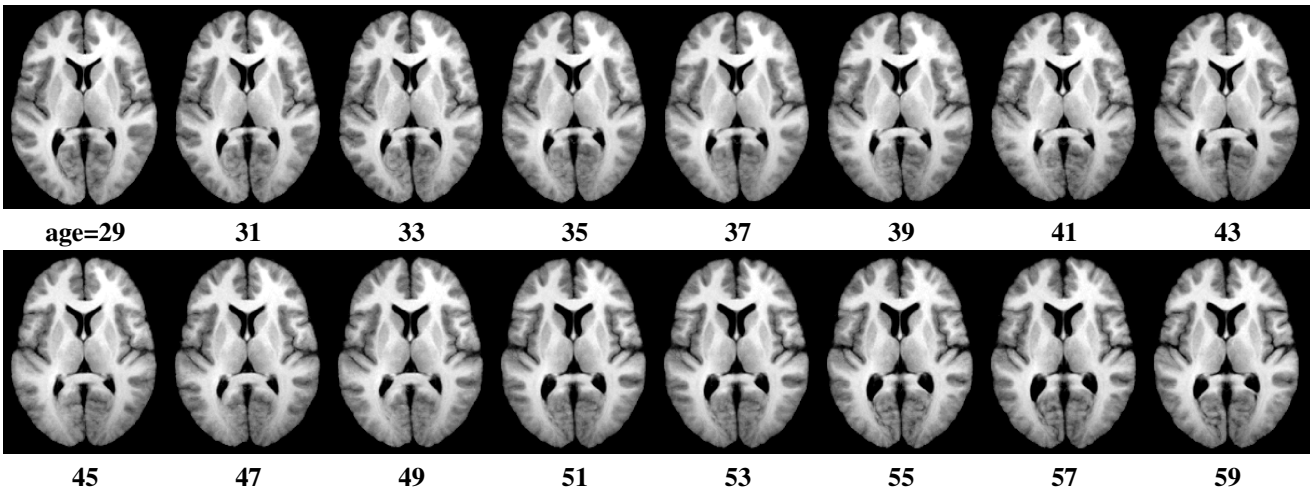

Figure 4. These images show the average brain shape as a function of age for the female cohort (ages noted below each image). These are not images from any particular patient—they are computed using the regression method proposed in this paper (14). Noticeable expansion of the lateral ventricles is clearly captured in both the image data and the determinant maps (Figure 5). All 2D slices are extracted from the 3D volumes that were used for computation.

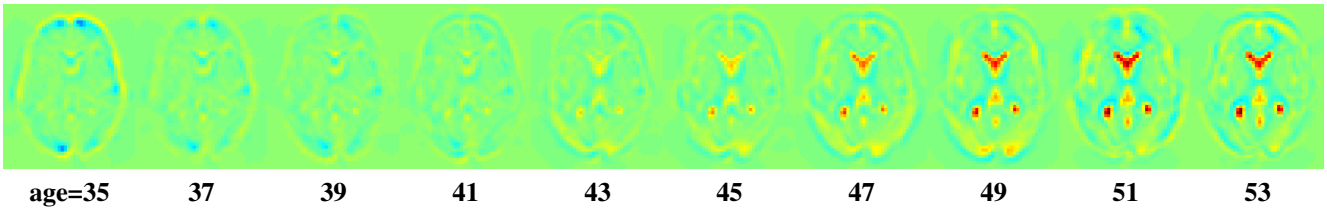

Figure 5. Illustration of the local brain shape change as a function of time for the female cohort. These data were generated by applying a diffeomorphic growth model to the representative images that were computed using manifold regression. Red indicates local expansion; blue indicates local contraction.

35, 41, 45, and 51 for the female cohort. More precisely, the figure shows the log-determinant of the Jacobian of the time-derivative of the deformation. In these images, red pixels indicate *expansion* of the underlying tissue, at the given age, while blue pixels indicate *contraction*. According to these determinant maps, expansion of the ventricles is evident for each age group. However, the expansion is accelerated for ages 45 to 53. Note that this finding agrees well with volume-based regression analysis from Figure 1.

4. Conclusion

We have proposed a method for *population shape regression* that enables novel analysis of population shape and growth from random design data when the underlying shape model is non-Euclidean. While the method is quite general, in this paper we apply this method to study the effect of aging on the brain. We regress a population representative shape, indexed by age, from a database of MR brain images. Finally, we apply a longitudinal growth model to these representative images to study the detailed local shape change that occurs, on average, as a function of age.

In the future, we plan to apply our method to a larger, more focused anatomical study. In terms of methodology, it is well known in the kernel regression community that kernel width plays a central role in determining the regression results [34]. We plan an extensive study of kernel width selection for our method.

5. Acknowledgements

We thank Bénédicte Mortamet for providing tissue volume data and Peter Lorenzen for image preprocessing. We greatfully acknowledge our funding sources including NIH grants R01 EB000219-NIH-NIBIB, R01 CA124608-NIH-NCI, and the National Alliance for Medical Image Computing (NAMIC), which is funded by the NIH Roadmap for Medical Research, Grant U54 EB005149.

References

[1] M. Beg, M. Miller, A. Trouvé, and L. Younes. Computing large deformation mettric mappings via geodesic flows

of diffeomorphisms. *International Journal of Computer Vision*, 61(2), February 2005. 4

[2] M. F. Beg. Variational and computational methods for flows of diffeomorphisms in image matching and growth in computational anatomy. *PhD thesis, The Johns Hopkins University*, 2003. 1

[3] R. Bhattacharya and V. Patrangenaru. Nonparametric estimation of location and dispersion on riemannian manifolds. *Journal of Statistical Planning and Inference*, 108:23–36, 2002. 2

[4] R. Bhattacharya and V. Patrangenaru. Large sample theory of intrinsic and extrinsic sample means on manifolds i. *Annals of Statistics*, 31(1):1–29, 2003. 2

[5] C. Bingham. An antipodally symmetric distribution on the sphere. *The Annals of Statistics*, 2(6):1201–1225, Nov 1974. 2

[6] S. R. Buss and J. P. Fillmore. Spherical averages and applications to spherical splines and interpolation. *ACM Transactions on Graphics*, 20(2):95–126, 2001. 3

[7] O. Clatz, M. Sermesant, P.-Y. Bondiau, H. Delingette, S. K. Warfield, G. Malandain, and N. Ayache. Realistic simulation of the 3D growth of brain tumors in MR images coupling diffusion with mass effect. *IEEE Transactions on Medical Imaging*, 24(10):1334–1346, October 2005. 1

[8] P. Dupuis and U. Grenander. Variational problems on flows of diffeomorphisms for image matching. *Quarterly of Applied Mathematics*, LVI(3):587–600, September 1998. 4

[9] P. T. Fletcher, S. Joshi, C. Ju, and S. M. Pizer. Principal geodesic analysis for the study of nonliner statistics of shape. *IEEE Transactions on Medical Imaging*, 23(8):995–1005, August 2004. 1, 2

[10] M. Frechet. Les elements aleatoires de nature quelconque dans un espace distancie. *Annales De L'Institut Henri Poincare*, 10:215–310, 1948. 2, 3

[11] U. Grenander and M. I. Miller. Computational anatomy: An emerging discipline. *Quarterly of Applied Mathematics*, 56(4):617–694, 1998. 1, 2, 4

[12] C. Guttmann, F. Jolesz, R. Kikinis, R. Killiany, M. Moss, T. Sandor, and M. Albert. White matter changes with normal aging. *Neurology*, 50(4):972–978, April 1998. 1

[13] W. Hardle. *Applied Nonparametric Regression*. Cambridge University Press, 1990. 1, 2

[14] S. Joshi, B. Davis, M. Jomier, and G. Gerig. Unbiased diffeomorphic atlas construction for computational anatomy. *NeuroImage (Supplemental issue on Mathematics in Brain Imaging)*, 23:S151–S160, 2004. 2, 4, 5

[15] S. C. Joshi and M. I. Miller. Landmark matching via large deformation diffeomorphisms. *IEEE Transactions On Image Processing*, 9(8):1357–1370, August 2000. 4

[16] P. Jupp and K. Mardia. A unified view of the theory of directional statistics, 1975–1988. *International Statistical Review*, 57(3):261–294, Dec 1989. 2

[17] P. E. Jupp and J. T. Kent. Fitting smooth paths to spherical data. *Applied Statistics*, 36(1):34–46, 1987. 2

[18] H. Karcher. Riemannian center of mass and mollifier smoothing. *Communications on Pure and Applied Mathematics*, 30:509–541, 1977. 3

[19] D. G. Kendall. Shape manifolds, Procrustean metrics, and complex projective spaces. *Bulletin of the London Mathematical Society*, 16:18–121, 1984. 2

[20] H. Le and D. Kendall. The riemannian structure of euclidean shape spaces: A novel environment for statistics. *The Annals of Statistics*, 21(3):1225–1271, Sep 1993. 2

[21] K. V. Leemput, F. Maes, D. Vandermeulen, and P. Suetens. Automated model-based tissue classification of mr images of the brain. *IEEE Transactions on Medical Imaging*, 18(10):897–908, October 1999. 3

[22] P. Lorenzen, M. Prastawa, B. Davis, G. Gerig, E. Bullitt, and S. Joshi. Multi-modal image set registration and atlas formation. *Medical Image Analysis*, 10(3):440–451, June 2006. 5

[23] M. Matsumae, R. Kikinis, I. Mórocz, A. Lorenzo, T. Sándor, T. Sándor, M. Albert, P. Black, and F. Jolesz. Age-related changes in intracranial compartment volumes in normal adults assessed by magnetic resonance imaging. *J Neurosurg*, 84:982–991, 1996. 1

[24] M. Miller. Computational anatomy: shape, growth, and atrophy comparison via diffeomorphisms. *NeuroImage*, 23:S19–S33, 2004. 1, 2, 5

[25] M. Miller, A. Banerjee, G. Christensen, S. Joshi, N. Khaneja, U. Grenander, and L. Matejic. Statistical methods in computational anatomy. *Statistical Methods in Medical Research*, 6:267–299, 1997. 4

[26] M. Miller and L. Younes. Group actions, homeomorphisms, and matching: A general framework. *International Journal of Computer Vision*, 41:61–84, January 2001. 2, 4

[27] M. I. Miller, A. Trouve, and L. Younes. On the metrics and euler-lagrange equations of computational anatomy. *Annual Review of Biomedical Engineering*, 4:375–405, 2002. 4

[28] B. Mortamet, D. Zeng, G. Gerig, M. Prastawa, and E. Bullitt. Effects of healthy aging measured by intracranial compartment volumes using a designed mr brain database. In *Lecture Notes in Computer Science (LNCS)*, volume 3749, pages 383–391. Medical Image Computing and Computer Assisted Intervention (MICCAI), 2005. 1, 3

[29] E. A. Nadaraya. On estimating regression. *Theory of Probability and its Applications*, 10:186–190, 1964. 2

[30] X. Pennec. Intrinsic statistics on riemannian manifolds: Basic tools for geometric measurements. *Journal of Mathematical Imaging and Vision*, 25:127–154, 2006. 2

[31] M. Prastawa, E. Bullitt, S. Ho, and G. Gerig. A brain tumor segmentation framework based on outlier detection. *Medical Image Analysis*, 8(3):275–283, 2004. 5

[32] P. M. Thompson, J. N. Giedd, R. P. Woods, D. MacDonald, A. C. Evans, and A. W. Toga. Growth patterns in the developing brain detected by using continuum mechanical tensor maps. *Nature*, 404(6774):190–193, March 2000. 1

[33] A. Trouvé and L. Younes. Metamorphoses through lie group action. *Foundations of Computational Mathematics*, 5(2):173–198, 2005. 4

[34] M. P. Wand and M. C. Jones. *Kernel Smoothing*. Number 60 in Monographs on Statistics and Applied Probabilitiy. Chapman & Hall/CRC, 1995. 1, 2, 6

[35] G. S. Watson. Smooth regression analysis. *Sankhya*, 26:101–116, 1964. 2